

Stability Analysis of a Nonlinear PID Controller

Yung-Deug Son, Sang-Do Bin, and Gang-Gyoo Jin*

Abstract: In our previous work, the authors presented an effective nonlinear proportional-integral-derivative (PID) controller by incorporating a nonlinear function. The proposed controller is based on a conventional PID control architecture, wherein a nonlinear gain is coupled in series with the integral action to scale the error. Three new tuning rules for processes represented as the first-order plus time delay (FOPTD) model were obtained by solving an optimization problem formulated to minimize three performance indices. The main feature of the proposed controller is that it preserves the numbers of tuning gains even though nonlinearity is introduced and remains easy implementation in real applications. However, due to the introduction of a nonlinear element, the stability problem of the proposed controller may be raised. This paper presents one sufficient condition in the frequency domain for the absolute stability of the nonlinear PID controller, based on circle stability theory. It is proved that the nonlinear gain used is in the sector $[0, 1]$. The condition of the linear block $F(s)$ is derived for the overall feedback system to be stable. Checking the stability and the effectiveness and robustness of the feedback system for setpoint tracking are demonstrated through a set of simulation works on three processes with uncertainty.

Keywords: Circle stability theory, FOPTD model, nonlinear PID controller, nonlinear gain, tuning rule.

1. INTRODUCTION

For over 70 years, the proportional-integral-derivative (PID) controller has been the most commonly used technique in the control field of both industry and academia. Due to its simple structure and good performance, the PID controller is by far dominating more than 90% of all control loops in process industries. Although the PID controller has relatively smaller parameters than other controllers do, the optimum tuning of its parameters is not a trivial task in the absence of a systematic approach. A variety of setting methods based on different PID controller structures including the well-known tuning methods of Ziegler and Nichols [1] have been proposed and most of them are summarized in the literature [2]. However, as industrial processes become more and more complex, time-varying, highly nonlinear or significant time delay characteristics inherited in processes lead to great difficulty in keeping the desired control performance of the PID controller. Many approaches have been suggested to improve the adaptability and robustness by employing the concepts of auto-tuning, self-tuning, adaptive or intelligent schemes. Some applications of these concepts, such

as relay feedback, self-tuning using pattern recognition, real-time adaptive tuning and intelligent methods combining with fuzzy logic, neural networks and evolutionary algorithms to PID controllers have been suggested in the literature [3–8]. Inspired by these, an attractive approach adopting nonlinearities within the framework of the PID controller and tuning parameters by using an evolutionary algorithm has been proposed in previous literature [9–19]. This approach can be roughly divided into employing nonlinearities to controller gains and scaling the error nonlinearly. The former nonlinear PID controllers achieve performance by gradually changing their gains based on error and/or error rate [9–15]. The latter nonlinear PID controllers, the other hand, achieve performance by scaling the error through a nonlinear gain in cascade with a linear PID controller [16–19]. However, due to the use of nonlinearities, most of them have the increased numbers of tuning parameters and it will impose a burden on industrial operators for their tuning. Through a previous work [17], the authors proposed a nonlinear PID controller which adopts a nonlinear gain in cascade with the integral term of the standard PID controller. Three new tuning rules for processes represented as the FOPTD model were then ob-

Manuscript received November 12, 2020; revised February 16, 2021 and March 1, 2021; accepted March 4, 2021. Recommended by Associate Editor Sung Jin Yoo under the direction of Editor Jessie (Ju H.) Park. This paper was supported by Education and Research promotion program of KOREATECH in 2021.

Yung-Deug Son is with Department of Mechanical Facility Control Engineering, Korea University of Technology and Education, 1600 Chungjeol-ro, Dongnam-gu, Cheonan-si, Chungcheongnam-do, Korea (e-mail: ydson@koreatech.ac.kr). Sang-Do Bin is with the Department of Mechatronics Engineering, Graduate School, Korea University of Technology and Education, 1600 Chungjeol-ro, Dongnam-gu, Cheonan, Chungnam 31253, Korea (e-mail: leo119103@gmail.com). Gang-Gyoo Jin is with the Department of Electrical Power and Control Engineering, Adama Science and Technology University, P.O. Box 1888, Ethiopia (e-mail: gjin30@gmail.com).

* Corresponding author.

tained by solving an optimization problem formulated to minimize three performance indices. The main advantages of the proposed controller lie in its easy implementation due to the use of a simple nonlinear gain and mitigation of the integrator windup due to scaling down a large input error of the integrator. As a succeeding study, it is of great significance to handle the stability problem of the proposed NPID controller under the uncertainties of process parameters. The useful tools for analysing the absolute stability of nonlinear systems include Popov criterion and circle criterion. Seraji derived simple expressions that relate the PI and PID controller gains and system parameters to the maximum allowable nonlinear gain using the Popov stability criterion [13]. The Popov stability criterion was used to determine the nonlinear gain to retain the stability of an enhanced PID control system [18]. The controller parameters were designed under assumptions of a sector bounded nonlinear gain, to a proper choice that satisfies the inequality of Popov [19]. As another method, Rezaei and Hashemzade [20] studied the absolute stability of nonlinear systems with generalized sector condition based on circle theorem.

In this paper, we present a method to analyse the absolute stability of the nonlinear PID controller for processes. By using circle theorem, we characterize a nonlinear function, and it provides explicit conditions to ensure the stability. The stability for uncertainties of the process model are also checked through the Nyquist band of the linear part transfer function. The effectiveness and robustness of the proposed controller for setpoint tracking is demonstrated through simulation on three processes. This paper is organized as follows: Section 2 gives a brief overview regarding the proposed nonlinear PID controller. Section 3 analyses the stability of the closed-loop system using circle theorem. Section 4 illustrates simulation results performed on three processes and discussion. Finally, conclusions are presented in Section 5.

2. NONLINEAR PID CONTROL SYSTEM

2.1. The nonlinear PID controller

Through the previous work [17], the authors proposed a nonlinear PID (NPID) controller which employs a simple nonlinear gain in cascade with the integral action of the standard PID controller. The closed-loop system including the NPID controller is shown in Fig. 1.

The NPID controller in the dotted box composes a linear proportional-derivative term and a nonlinear integral term; $G_p(s)$ the process transfer function; y_s , y and u the setpoint (SP) signal, the process variable (PV) and the control signal, respectively; e the error ($e = \text{SP} - \text{PV}$).

The time-domain equation of the NPID controller is

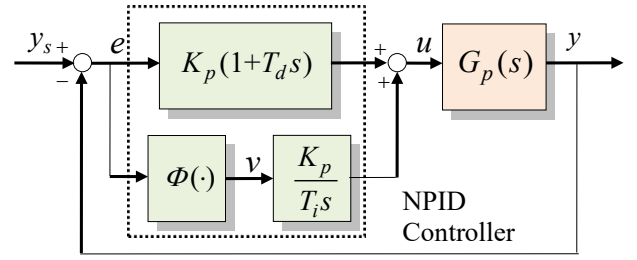


Fig. 1. The NPID control system.

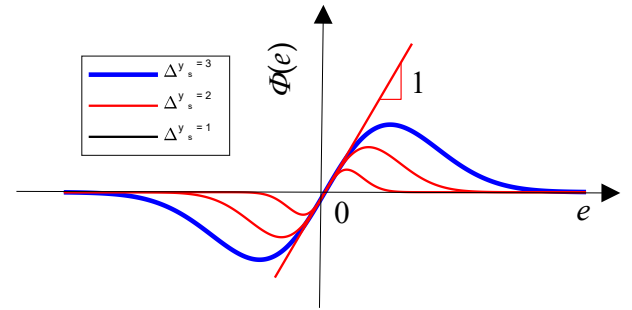


Fig. 2. Shapes of $\Phi(e)$ versus e according the change of y_s .

given by

$$u(t) = K_p \left[e(t) + \frac{1}{T_i} \int v(t) dt + T_d \frac{de(t)}{dt} \right], \quad (1)$$

where K_p , T_i and T_d denote the proportional gain, the integral time and the derivative time, respectively. $v(t)$ is a scaled error defined as

$$v(t) = \Phi(e) = k(e)e(t), \quad (2)$$

where $\Phi(e)$ is a nonlinear function of $e(t)$ that is introduced to improve the performance of the closed-loop system. $k(e)$ is a nonlinear gain defined as follows:

$$k(e) = \exp\left(-\frac{e^2}{2\Delta y_s^2}\right), \quad (3)$$

where $\Delta y_s (\neq 0)$ denotes the difference between the current SP and the previous SP. The typical plots of $\Phi(e)$ for $\Delta y_s = 1, 2$, and 3 are shown in Fig. 2. Note that the place to which this nonlinearity is applied is the integral term. The main advantages of this formulation is that the large error is scaled down near to zero by adopting $k(e)$ as the conditional integration anti-windup technique [22] sets the integrator off when the error exceeds a pre-set level. Consequently, with this NPID controller, integrator windup can be mitigated to some extent.

Table 1. Tuning rules for step setpoint tracking based on ISE, IAE and ITAE ($0.01 \leq L/\tau < 1$).

Performance Index	Dimensionless parameters		
	KK_p	T_i/τ	T_d/τ
ISE	$1.2886(\frac{L}{\tau})^{-0.9182}$	$0.9217 + 0.2375\frac{L}{\tau}$	$0.4302(\frac{L}{\tau})^{0.9645}$
IAE	$1.0350(\frac{L}{\tau})^{-0.9327}$	$0.9465 + 0.1398\frac{L}{\tau}$	$0.3527(\frac{L}{\tau})^{0.9406}$
ITAE	$1.0019(\frac{L}{\tau})^{-0.9457}$	$0.8723 + 0.1848\frac{L}{\tau}$	$0.3401(\frac{L}{\tau})^{0.9799}$

Table 2. Tuning rules for step setpoint tracking based on ISE, IAE and ITAE ($1 \leq L/\tau \leq 3$).

Performance Index	Dimensionless parameters		
	KK_p	T_i/τ	T_d/τ
ISE	$1.3362(\frac{L}{\tau})^{-0.5488}$	$0.8419 + 0.3190\frac{L}{\tau}$	$0.4137(\frac{L}{\tau})^{0.75}$
IAE	$1.0822(\frac{L}{\tau})^{-0.5495}$	$0.8237 + 0.2692\frac{L}{\tau}$	$0.3331(\frac{L}{\tau})^{0.6831}$
ITAE	$1.0093(\frac{L}{\tau})^{-0.5198}$	$0.7813 + 0.2781\frac{L}{\tau}$	$0.2878(\frac{L}{\tau})^{0.7317}$

2.2. Tuning rules of the NPID controller

Many industrial processes can be represented by the FOPTD model as

$$G_p(s) = \frac{Ke^{-Ls}}{\tau s + 1}, \quad (4)$$

where K denotes the steady-state gain, τ the time constant, and L the dead time of the process. Three parameters may change within the upper and lower bounds as

$$\begin{aligned} K_{lower} &\leq K \leq K_{upper}, \\ \tau_{lower} &\leq \tau \leq \tau_{upper}, \\ L_{lower} &\leq L \leq L_{upper}. \end{aligned} \quad (5)$$

By using dimensionless analysis, a genetic algorithm (GA) and the least squares method, the authors proposed three tuning rules. The tuning rules were obtained such that the overall closed-loop response minimizes one of the following performance indices: integral of the square value of the error (ISE), integral of the absolute value of the error (IAE), and integral of the time weighted absolute value of the error (ITAE). The results are listed in Tables 1-2.

3. STABILITY ANALYSIS OF THE NPID CONTROL SYSTEM

Since adopting a nonlinear gain in the structure of the proposed controller, stability analysis of the overall control system is necessary.

For this purpose, circle stability theory is applied. Let us consider a nonlinear closed-loop system which can decompose a linear block $F(s)$ and a nonlinear block Φ as shown in Fig. 3. Here, y_s is assumed to be zero or a constant without loss of generality.

Definition 1: A memoryless function $\Phi: \mathfrak{R} \rightarrow \mathfrak{R}$ is said to belong to the sector $[k_1, k_2]$, if there are constants α, β, k_1 and k_2 (with $0 \leq k_1 < k_2$ and $\alpha < 0 < \beta$) such that

$$k_1 e^2 \leq \Phi(e)e \leq k_2 e^2 \text{ for } \forall e \in [\alpha, \beta]. \quad (6)$$

Definition 1 implies $\Phi(0) = 0$ and $\Phi(e)e \geq 0$. This means that $\Phi(e)$ lies in between two straight lines $k_1 e$ and $k_2 e$, that is, in the first and third quadrants as shown in Fig. 4. If (6) holds for all $e \in (-\infty, \infty)$, it is said that the sector condition holds globally.

Theorem 1: Consider the system in Fig. 3 where $F(s)$ is stable (i.e., it has all its poles in the left half-plane with one pole at the origin) and Φ satisfies the sector condition (6) globally.

Then, the system is absolutely stable if the following condition is satisfied:

$$\operatorname{Re} \left[\frac{1 + k_2 F(i\omega)}{1 + k_1 F(i\omega)} \right] > 0, \quad \omega \in \mathfrak{R}. \quad (7)$$

Proof: Theorem 1 can be proved by using loop transformation, a Lyapunov function and the Kalman-Yakubovich-Popov equations. See [23].

Lemma 1: Consider the system shown in Fig. 3. Then, it is absolutely stable if the following condition is satisfied:

If $0 = k_1 < k_2$, $F(s)$ is stable and the Nyquist plot of $F(i\omega)$ lies in the plane $\{s \in \mathbb{C} \mid \operatorname{Re}(s) > -1/k_2\}$.

Proof: Suppose that $F(i\omega) = \alpha + i\beta$. Then, with $k_1 = 0$, (7) can be rewritten as

$$\begin{aligned} \operatorname{Re} [1 + k_2 F(i\omega)] &= \operatorname{Re} [1 + k_2(\alpha + i\beta)] \\ &= 1 + k_2 \alpha > 0. \end{aligned}$$

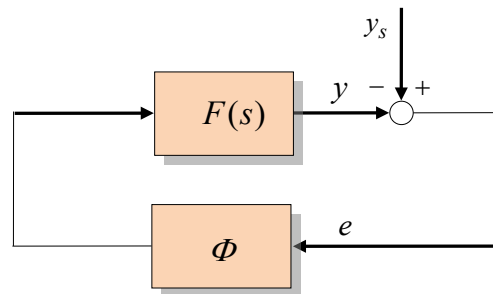


Fig. 3. A nonlinear feedback system.

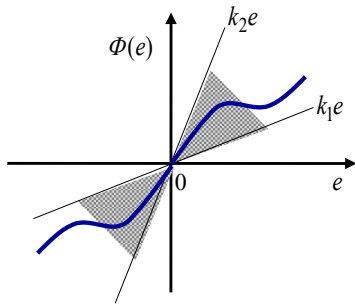


Fig. 4. Sector-bounded nonlinearity $\Phi(e)$.

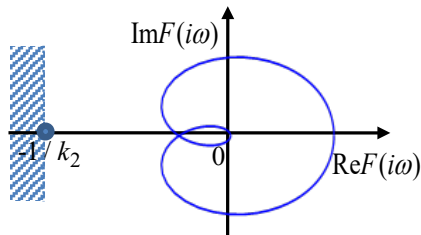


Fig. 5. Nyquist plot of $F(i\omega)$.

Rearranging the above inequality yields

$$\text{Re}F(i\omega) = \alpha > -1/k_2. \tag{8}$$

This inequality implies that the Nyquist plot of $F(i\omega)$ is located on the right of a vertical line defined by $\text{Re}F(i\omega) = -1/k_2$. Fig. 5 shows the Nyquist plot of $F(i\omega)$ along with its forbidden region.

Let us now consider the NPID control system shown in Fig. 1. After some manipulation of the block diagram, it can be decomposed into the linear and nonlinear blocks as in Fig. 3. Then, the linear-part transfer function $F(s)$ is written by

$$F(s) = \frac{K_p G_p(s)}{T_i s [1 + K_p (1 + T_d s) G_p(s)]}. \tag{9}$$

If $G_p(s)$ possesses time delay, time delay can be approximated by a rational transfer function using the second-order Padé approximation as

$$e^{-Ls} = \frac{s^2 - \frac{6}{L}s + \frac{12}{L^2}}{s^2 + \frac{6}{L}s + \frac{12}{L^2}}. \tag{10}$$

Theorem 2: Consider the nonlinear function in (2). $\Phi(e)$ belongs to the sector $[0,1]$.

Proof: From the fact that the nonlinear gain (3) is an even function, clearly we have

$$k(e) = k_1 = 0 \text{ as } e \rightarrow \infty \text{ or } e \rightarrow -\infty,$$

and also

$$k(e) = k_2 = 1 \text{ as } e = 0.$$

Since we have $0 \leq \Phi(e)e \leq e^2$ for $\forall e \in \mathfrak{R}$, $\Phi(e)$ belongs to the sector $[0, 1]$.

Consequently, according to Lemma 1, the system in Fig. 1 becomes absolutely stable if $F(s)$ is stable since Φ is in the sector $[0, 1]$. In other words, the NPID control system is absolutely stable if $F(s)$ has all its poles in the left half-plane with one pole at the origin. Therefore, we will examine this condition in detail through example processes in the next section.

4. SIMULATION RESULTS

This section illustrates the effectiveness of the proposed controller setting for minimizing the IAE performance index and assesses the absolute stability of the closed-loop system over three processes taken from the literature. The responses of the NPID controller are compared with those of the linear PID controller tuned by the ASP method [24], the SL method [25], the YXC method [26], and the IMC method [27]. The abbreviations of ‘ASP’ for Anwar, Shamsuzzoha and Pan, ‘SL’ for Shamsuzzoha and Lee, and ‘YXC’ for Yang, Xu and Chiu are used, respectively.

4.1. Process 1

A FOPTD process is considered from [24] as given by

$$G_p(s) = \frac{K_0 e^{-L_0 s}}{\tau_0 s + 1}. \tag{11}$$

The nominal parameter values of this process are $K_0 = 1$, $\tau_0 = 1$, and $L_0 = 0.5$ but in this work each parameter is considered to vary within the 20% range from its nominal value. The ranges of variation result in $0.8 \leq K_0 \leq 1.2$, $0.8 \leq \tau_0 \leq 1.2$, and $0.4 \leq L_0 \leq 0.6$. Table 3 lists the settings of the PID controller and the NPID controller for the nominal process.

In order to check the absolute stability of the NPID control system, $F(s)$ is obtained through (9) to (11) as

$$F(s) = \frac{b_1 s^2 + b_2 s + b_3}{s(a_0 s^3 + a_1 s^2 + a_2 s + a_3)}, \tag{12}$$

where

$$b_1 = \frac{KK_p}{T_i}, b_2 = -\frac{6KK_p}{LT_i}, b_3 = \frac{12KK_p}{L^2 T_i},$$

$$a_0 = \tau + KK_p T_d,$$

Table 3. Controller settings for Process 1.

Method	Gains		
	K_p	K_i	K_d
NPID	1.976	1.944	0.363
PID-ASP	1.12	1.0	0.12
PID-SL	1.08	1.02	0.11
PID-IMC	1.11	0.88	0.11

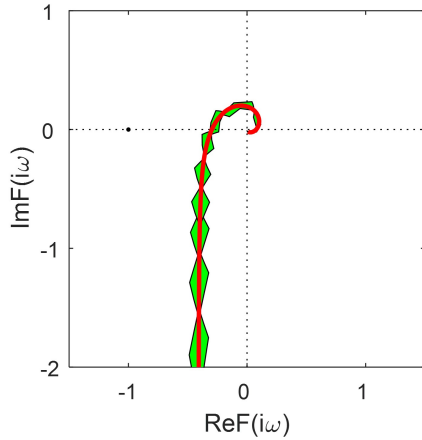


Fig. 6. Nyquist diagram and Nyquist band of $F(i\omega)$ for Process 1.

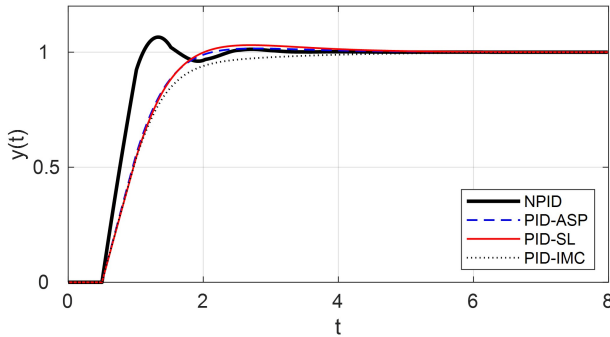


Fig. 7. Responses for the unit step input on Process 1.

$$a_1 = 1 + KK_p + \frac{6\tau}{L} - \frac{6KK_pT_d}{L},$$

$$a_2 = \frac{6}{L} + \frac{12\tau}{L^2} - \frac{6KK_p}{L} + \frac{12KK_pT_d}{L^2},$$

$$a_3 = \frac{12}{L^2} + \frac{12KK_p}{L^2}.$$

With the nominal parameter values and the NPID controller settings, the denominator equation of $F(s)$, $s(s^3 + 7.7906s^2 + 39.4106s + 104.788) = 0$, gives 4 poles of 0, -2.5940 , $-3 \pm 1.7321i$. Therefore, the closed-loop system becomes absolutely stable according to Lemma 1. In order to examine this fact graphically, we plotted the Nyquist diagram (red color) as well as the Nyquist band (green color) in the variation range of the process parameters. It can be seen in Fig. 6 that as well as the Nyquist diagram, the Nyquist band lies to the right of a vertical line of $\text{Re}F(i\omega) = -1/k_2 = -1$.

To evaluate the SP tracking performance of the NPID controller, the responses for a unit step SP change were obtained with those of the ASP method, the SL method, and the IMC method. The responses in Fig. 7 clearly shows that the NPID controller provides moderately larger overshoot but it produces good transient responses.

For a quantitative comparison of the responses, the per-

Table 4. Performance indices of the SP tracking responses for Process 1.

Method	t_r	M_p	t_s	IAE
NPID	0.515	6.540	2.185	0.818
PID-ASP	1.201	1.609	1.925	1.051
PID-SL	1.185	3.050	3.537	1.084
PID-IMC	1.577	-	3.147	1.126

formance indices such as rise time t_r ($= t_{0.95} - t_{0.05}$), overshoot M_p , 2% settling time t_s , and IAE were obtained. They are summarized in Table 4.

It is observed that the NPID controller offers relatively larger M_p but not too big at the expense of enhancing the swiftness of response than the others.

4.2. Process 2

A fifth-order plus dead-time process is considered [24] where the process has transfer function as

$$G_p(s) = \frac{K_0 e^{-L_0 s}}{(\tau_0 s + 1)^3 (s + 1)^2}. \quad (13)$$

The nominal parameter values of this process are $K_0 = 1$, $\tau_0 = 2$, and $L_0 = 8$. It is assumed that each parameter varies within the ranges of $0.8 \leq K_0 \leq 1.2$, $1.6 \leq \tau_0 \leq 2.4$, and $6.4 \leq L_0 \leq 9.6$. The FOPTD model of Process 2 was determined by using a GA-based model reduction technique. An input was simultaneously applied to both the process and the parallel-connected FOPTD model. The model parameters K , τ , and L were adjusted by a GA to minimize a performance index of the difference between the process output and the model output. This technique results in $K = 1$, $\tau = 4.119$, and $L = 12.230$ and $L/\tau \approx 2.97$ in this process. The settings of the PID controller tuned by the ASP method [24], the YXC method [26] and the IMC method [27] and the NPID controller are listed in Table 5.

As the previous example, in order to examine the absolute stability of the closed-loop system, $F(s)$ can be written as follows:

$$F(s) = \frac{b_5 s^2 + b_6 s + b_7}{s(a_0 s^7 + a_1 s^6 + a_2 s^5 + a_3 s^4 + a_4 s^3 + a_5 s^2 + a_6 s + a_7)}, \quad (14)$$

Table 5. Controller settings for Process 2.

Method	Gains		
	K_p	K_i	K_d
NPID	0.595	0.089	1.717
PID-ASP	0.543	0.055	2.30
PID-SL	0.63	0.060	1.745
PID-IMC	0.56	0.063	1.316

Table 6. Performance indices of the SP tracking responses for Process 2.

Method	t_r	M_p	t_s	IAE
NPID	12.018	4.239	34.281	17.618
PID-ASP	13.531	1.913	43.589	18.647
PID-SL	10.638	10.779	50.593	18.489
PID-IMC	11.227	13.723	52.776	18.936

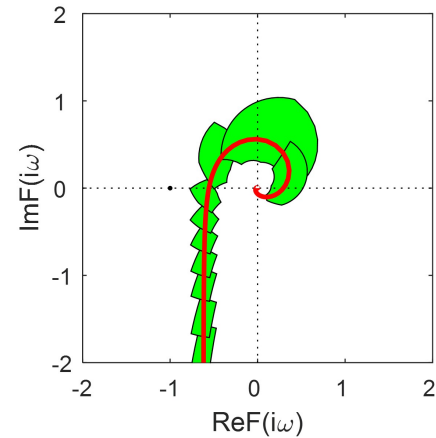
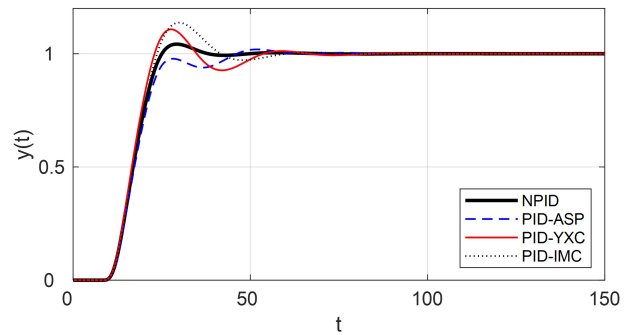
where

$$\begin{aligned}
 b_5 &= \frac{KK_p}{T_i}, \quad b_6 = -\frac{6KK_p}{LT_i}, \quad b_7 = \frac{12KK_p}{L^2T_i}, \\
 a_0 &= \tau^3, \\
 a_1 &= \frac{6\tau^3}{L} + 2\tau^3 + 3\tau^2, \\
 a_2 &= \frac{12\tau^3}{L^2} + \frac{6}{L}(2\tau^3 + 3\tau^2) + \tau^3 + 6\tau^2 + 3\tau, \\
 a_3 &= \frac{12}{L^2}(2\tau^3 + 3\tau^2) + \frac{6}{L}(\tau^3 + 6\tau^2 + 3\tau) + 3\tau^2 \\
 &\quad + 6\tau + 1, \\
 a_4 &= \frac{12}{L^2}(\tau^3 + 6\tau^2 + 3\tau) + \frac{6}{L}(3\tau^2 + 6\tau + 1) + 3\tau \\
 &\quad + 2 + K_p T_d, \\
 a_5 &= \frac{12}{L^2}(3\tau^2 + 6\tau + 1) + \frac{6}{L}(3\tau + 2) + 1 + KK_p \\
 &\quad - \frac{6KK_d}{L}, \\
 a_6 &= \frac{12}{L^2}(3\tau + 2) + \frac{6}{L} - \frac{6KK_p}{L} + \frac{12KK_d}{L^2}, \\
 a_7 &= \frac{12}{L^2} + \frac{12KK_p}{L^2}.
 \end{aligned}$$

Since the denominator of $F(s)$ has 8 stable poles of $-1.457 \pm 0.536i$, $-0.439 \pm 0.754i$, -0.347 , $-0.055 \pm 0.236i$ and 0, it is also absolutely stable according to Lemma 1. We plotted the Nyquist band in the variation range of the process parameters as well as the Nyquist diagram with changing ω . It can be seen in Fig. 8 that they lies to the right of a vertical line of $\text{Re}F(i\omega) = -1$.

Fig. 9 depicts the unit step responses of the four methods. As shown in Fig. 9, the ASP method exhibits a sluggish response whereas the YXC method does an oscillatory response. The response obtained using the proposed method shows smaller overshoot, remarkably reduced settling time and IAE than the other methods.

Comparison of the PID and NPID controller settings in Table 6 shows that the proposed method provides more improved quantitative performance indices.


Fig. 8. Nyquist diagram and Nyquist band of $F(i\omega)$ for Process 2.

Fig. 9. Responses for the unit step input on Process 2.

4.3. Process 3

Consider a twentieth-order process model without time delay as follows [24]:

$$G_p(s) = \frac{K_0}{(\tau_0 s + 1)^{20}}. \quad (15)$$

The nominal parameter values of this process are $K_0 = 1$, and $\tau_0 = 1$ and two parameters can vary within the ranges of $0.8 \leq K_0$ and $\tau_0 \leq 1.2$. In the case of Process 3, consequently $K = 1.0$, $\tau = 7.389$, $L = 13.598$ were estimated as the FOPDT model and $L/\tau \approx 1.84$. The settings of the PID controllers and the NPID controller are summarized in Table 7.

Since the denominator of $F(s)$ has stable 21 poles of

Table 7. Controller settings for Process 3.

Method	Gains		
	K_p	K_i	K_d
NPID	0.615	0.074	2.598
PID-ASP	0.525	0.055	1.66
PID-SL	0.62	0.052	2.21
PID-IMC	0.55	0.05	1.87

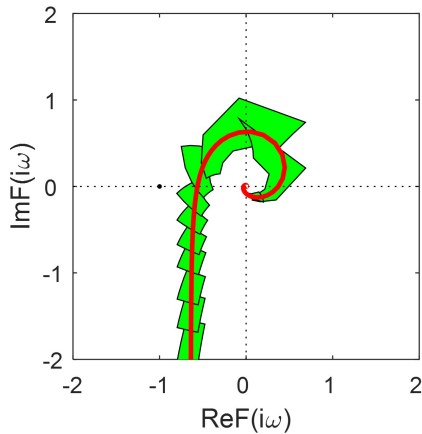


Fig. 10. Nyquist diagram and Nyquist band of $F(i\omega)$ for Process 3.

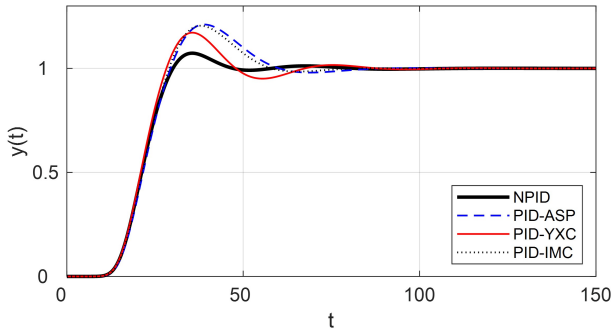


Fig. 11. Responses for the unit step input on Process 3.

Table 8. Performance indices of the SP tracking responses for Process 2.

Method	t_r	M_p	t_s	IAE
NPID	14.679	7.311	43.688	22.283
PID-ASP	14.246	21.091	69.432	25.541
PID-SL	13.376	17.183	63.409	23.774
PID-IMC	13.914	20.508	55.020	24.852

-2.082 , $-2.025 \pm 0.344i$, $-1.860 \pm 0.651i$, $-1.607 \pm 0.887i$, $-1.291 \pm 1.029i$, -0.238 , $-0.948 \pm 1.061i$, $-0.616 \pm 0.979i$, $-0.331 \pm 0.793i$, $-0.128 \pm 0.522i$, $-0.035 \pm 0.191i$ and 0 , it also becomes absolutely stable according to Lemma 1. It can be seen in Fig. 10 that both the Nyquist diagram and the Nyquist band lie to the right of a vertical line of $\text{Re}F(i\omega) = -1$. The unit step responses obtained using the four methods were compared in Fig. 11 and the performance indices are listed in Table 8. A clear enhancement in the responses is observed from Fig. 11. The response of the NPID controller exhibits relatively smaller overshoot, shorter settling time and smaller IAE than those using the PID controller.

5. CONCLUSION

The authors proposed a NPID controller comprised of a simple nonlinear gain in cascade with the integral term of the conventional PID controller. The three model-based tuning rules for processes represented by a FOPTD model were introduced. In this paper, the stability of the closed-loop system incorporating the NPID controller was investigated using the circle criterion. Since the nonlinear gain $k(e)$ used in this paper belongs to the sector $[0, 1]$, a sufficient condition for the closed-loop system to be absolutely stable is that the linear block $F(s)$ has all its poles in the left half-plane with one pole at the origin. Three numerical examples were provided to demonstrate the efficiency of the proposed method. The simulation results have shown that each linear block $F(s)$ with the associated NPID controller settings is stable. An IAE comparison results clearly indicated that the proposed method gives consistently better performances than the linear PID controllers tuned by the other three methods. In the future work, we will further conduct a comparative study with other nonlinear PID control methods.

REFERENCES

- [1] J. G. Ziegler and N. B. Nichols, "Optimum setting for automatic controllers," *ASME Trans*, vol. 64, no. 8, pp. 759-768, November 1942.
- [2] A. O'Dwyer, *Handbook of PI and PID Controller Tuning Rules*, 2nd ed., Imperial College Press, pp. 154-180, 2006.
- [3] K. J. Åström and T. Hägglund, "Automatic tuning of simple regulators with specification of phase and amplitude margins," *Automatica*, vol. 20, no. 5, pp. 645-651, April 1984.
- [4] S. M. Girirajkumar, A. A. Kumar, and N. Anantharaman, "Tuning of a PID controller for a real time industrial process using particle swarm optimization," *Int. J. of Computer Applications*, vol. 1, no. 7, pp. 35-40, December 2010.
- [5] J.-W. Perng, Y.-C. Kuo, and K.-C. Lu, "Design of the PID controller for hydro-turbines based on optimization algorithms," *International Journal of Control, Automation, and Systems*, vol. 18, no. 7, pp. 1758-1770, 2020.
- [6] A. A. Khan and N. Rapal, "Fuzzy PID controller design, tuning and comparison with conventional PID controller," *Proceedings of IEEE Int. Conf. on Engineering of Intelligent Systems*, pp. 1-6, 2006.
- [7] R. Kumar, S. Srivastava, and J. R. P. Gupta, "Artificial neural network based PID controller for online control of dynamical systems," *Proceedings of the 1st IEEE Int. Conf. on Power Electronics, Intelligent Control and Energy Systems*, pp. 1-6, 2016.
- [8] K. Li, S. Boonto, and T. Nuchkrua, "On-line self tuning of contouring control for high accuracy robot manipulators under various operations," *International Journal of Control, Automation, and Systems*, vol. 18, no. 7, pp. 1818-1828, 2020.

- [9] B. M. Slayed and M. A. Hawwa, "A nonlinear PID control scheme for hard disk drive servo systems," *Proceedings of Mediterranean Conf. on Control and Automation*, pp. 1-6, 2007.
- [10] M. Korkmaz, O. Aydogdu, and H. Dogan, "Design and performance comparison of variable parameter nonlinear PID controller and genetic algorithm based PID controller," *Proceedings of IEEE Int. Symp. on Innovations in Intelligent Systems and Applications*, pp. 1-5, 2012.
- [11] H. Zhang and B. Hu, "The application of nonlinear PID controller in generator excitation system," *Energy Procedia*, vol. 17, Part A, pp. 202-207, 2012.
- [12] G. B. So and G. G. Jin, "Fuzzy-based nonlinear PID controller and its application to CSTR," *Korean Journal of Chemical Engineering*, vol. 35, no. 4, pp. 819-825, April 2018.
- [13] H. Seraji, "A new class of nonlinear PID controllers with robotic applications," *Journal of Robotic Systems*, vol. 15, no. 3, pp. 161-181, December 1998.
- [14] D. Kler, K. P. S. Rana, and V. Kumar, "A nonlinear PID controller based novel maximum power point tracker for PV systems," *Journal of the Franklin Institute*, vol. 335, no. 16, pp. 7828-7864, June 2018.
- [15] C. Zheng, Y. Su, and P. Mercorelli, "A simple nonlinear PD control for faster and high-precision positioning of servomechanisms with actuator saturation," *Mechanical Systems and Signal Processing*, vol. 121, no. 15, pp. 215-226, April 2019.
- [16] G. B. So, H. S. Yi, Y. D. Son, and G. G. Jin, "Temperature control of a regasification system for LNG-fuelled marine engines using nonlinear control techniques," *Int. Journal of Control, Automation and Systems*, vol. 16, no. 6, pp. 3047-3054, October 2018.
- [17] G. G. Jin and Y. D. Son, "Design of a nonlinear PID controller and tuning rules for first-order plus time delay models," *Studies in Informatics and Control*, vol. 28, no. 2, pp. 157-166, July 2019.
- [18] Y. X. Su, D. Sun, and B. Y. Duan, "Design of an enhanced nonlinear PID controller," *Mechatronics*, vol. 15, no. 8, pp. 1005-1024, October 2005.
- [19] A. Maddi, A. Guessoum, and D. Berkani, "Design of nonlinear PID controllers based on hyper-stability criteria," *Proceedings of 15th Int. Conf. on Sciences and Techniques of Automatic Control*, pp. 21-23, 2014.
- [20] A. Rezaei and F. Hashemzade, "Absolute stability of nonlinear systems with piecewise linear sector condition," *Int. J. of Computer Applications*, vol. 134, no. 9, pp. 15-18, January 2016.
- [21] V. Vijayan, S. Narayanan, P. Kanagasabapathy, and J. Prakash, "Stability analysis of first order plus time delay system under PI & PID control for simultaneous parameter variation," *Proc. of Annual IEEE India Conference*, pp. 73-77, 2005.
- [22] L. Rundqwist, *Anti-reset Windup for PID Controllers*, Ph.D. Thesis, Department of Automatic Control, Lund Inst. of Technology, Sweden, 1991.
- [23] W. M. Haddad and V. Chellaboina, *Nonlinear Dynamical Systems and Control: A Lyapunov-Based Approach*, Princeton University Press, pp. 372-387, 2007.
- [24] M. N. Anwar, M. Shamsuzzoha, and S. Pan, "A frequency domain PID controller design method using direct synthesis approach," *Arab J. Sci. Eng.*, vol. 40, pp. 995-1004, February 2015.
- [25] M. Shamsuzzoha and M. Lee, "IMC-PID controller design for improved disturbance rejection of time-delayed processes," *Ind. Eng. Chem. Res.*, vol. 46, no. 7, pp. 2077-2091, March 2007.
- [26] X. Yang, Bu Xu, and M. S. Chiu, "PID controller design directly from plant data," *Ind. Eng. Chem. Res.*, vol. 50, no. 3, pp. 1352-1359, February 2011.
- [27] W. Zhang, Y. Xi, G. Yang, and X. Xu, "Design PID controllers for desired time-domain or frequency-domain response," *ISA Trans.*, vol. 41, no. 4, pp. 511-520, October 2002.



Yung-Deug Son received his B.S. degree in control and instrumentation engineering from Korea Maritime University in 1997. He was a student researcher with Tokyo Institute of Technology, Japan, in 1998, and received an M.S. degree in from Kobe University of Mercantile Ocean Electro-Mechanical, Japan, in 2001, and a Ph.D. degree from the Department of Electrical Engineering, from Pusan National University, Busan, Korea, in 2015, respectively. From 2001 to 2009, he was a Senior Research Engineer with Hyundai Heavy Industries Co., Ltd. He has been with the School of Mechanical Facility Control Engineering, Korea University of Technology and Education (KOREATECH), where he is currently an assistant professor. His research interests include power conversion, electric machine drives and intelligent control.



Sang-Do Bin received his B.S. and M.S. degrees in marine engineering from Korea Maritime University, in 1983 and 2013, respectively. He is currently working toward a Ph.D. degree in the Department of Mechatronics Engineering, Korea University of Technology and Education (KOREATECH). His research interests include intelligent control and optimization using generalized predictive control algorithms.



Gang-Gyoo Jin received his B.S. degree in marine engineering from Korea Maritime University and an M.S. degree in electrical, electronic and computer engineering from Florida Institute of Technology and a Ph.D. degree in electrical, electronic and system engineering from University of Wales Cardiff, in 1977, 1985, and 1996, respectively. His research inter-

ests include intelligent control, fractal technique, and optimization using genetic algorithms.

Publisher's Note Springer Nature remains neutral with regard to jurisdictional claims in published maps and institutional affiliations.